Nonapical and Cytoplasmic Expression of Interleukin-8, CXCR1, and CXCR2 Correlates with Cell Proliferation and Microvessel Density in Prostate Cancer

Catherine Murphy,[1] Maryalice McGurk,[1] Johanna Pettigrew,[1] Alfredo Santinelli,[2] Roberta Mazzucchelli,[2] Patrick G. Johnston,[1] Rodolfo Montironi,[2] and David J.J. Waugh[1]

Abstract

Purpose: We characterized interleukin-8 (IL-8) and IL-8 receptor expression (CXCR1 and CXCR2) in prostate cancer to address their significance to this disease.

Experimental Design: Immunohistochemistry was conducted on 40 cases of human prostate biopsy containing histologically normal and neoplastic tissue, excised from patients with locally confined or invasive androgen-dependent prostate cancer, and 10 cases of transurethral resection of the prostate material from patients with androgen-independent disease.

Results: Weak to moderate IL-8 expression was strictly localized to the apical membrane of normal prostate epithelium. In contrast, membranous expression of IL-8, CXCR1, and CXCR2 was nonapical in cancer cells of Gleason pattern 3 and 4, whereas circumferential expression was present in Gleason pattern 5 and androgen-independent prostate cancer. Each of IL-8, CXCR1, and CXCR2 were also increasingly localized to the cytoplasm of cancer cells in correlation with advancing stage of disease. Cytoplasmic expression (but not apical membrane expression) of IL-8 in Gleason pattern 3 and 4 cancer correlated with Ki-67 expression ($R = 0.79$; $P < 0.001$), cyclin D1 expression ($R = 0.79$; $P < 0.001$), and microvessel density ($R = 0.81$; $P < 0.001$). *In vitro* studies on androgen-independent PC3 cells confirmed the mitogenic activity of IL-8, increasing the rate of cell proliferation through activation of both CXCR1 and CXCR2 receptors.

Conclusions: We propose that the concurrent increase in IL-8 and IL-8 receptor expression in human prostate cancer induces autocrine signaling that may be functionally significant in initiating and promoting the progression of prostate cancer by underpinning cell proliferation and angiogenesis.

Expression of the CXC chemokine, interleukin-8 (IL-8), in prostate cancer cells has been shown to correlate with the angiogenesis, tumorigenicity, and metastasis of experimental prostate cancer in athymic nude mice (1, 2). These *in vivo* observations are supported by *in vitro* experimentation demonstrating that IL-8 increases the invasiveness of prostate cancer cells through regulation of matrix metalloproteinase synthesis and secretion (1–3) and underpins the progression toward androgen-independent growth of the LNCaP cell line (4). Furthermore, clinical studies have reported an increased expression of IL-8 in the serum of prostate cancer patients over that of normal subjects or patients with benign prostatic hypertrophy (5). In addition, genetic studies have reported that the frequency of a specific polymorphism in the IL-8 gene promoter that results in elevated IL-8 expression is more prevalent in patients with metastatic prostate cancer compared with normal controls (6). Despite the above studies implicating IL-8 expression in the metastasis of human prostate cancer, the true functional significance of IL-8 within the multiple steps of the metastatic cascade is poorly understood and hindered by the absence of pathologic examination of its expression in normal and neoplastic prostate tissue. Furthermore, the expression and functional significance of the two IL-8 receptors, CXCR1 and CXCR2, in promoting disease progression has not been extensively studied.

The aim of the current study was to characterize the intensity and distribution of IL-8 and IL-8 receptor expression in increasing stages of human prostate cancer using immunohistochemistry on needle core prostate biopsy or transurethral resection of the prostate material. Through correlative analysis with markers of cell proliferation and angiogenesis *in vivo* and *in vitro* studies, we now provide additional evidence to support a role for IL-8 in human prostate cancer progression by underpinning prostate cancer cell proliferation and angiogenesis.

Authors' Affiliations: [1]Centre for Cancer Research and Cell Biology, Queens University Belfast, Belfast, Northern Ireland and [2]Section of Pathological Anatomy and Histopathology, Polytechnic University of the Marche Region (Ancona), Ancona, Italy

Received 7/30/04; revised 10/20/04; accepted 10/29/04.

Grant support: Ulster Cancer Foundation (P.G. Johnston and D.J.J. Waugh), Royal Society (D.J.J. Waugh), Northern Ireland HPSS R&D Office (D.J.J. Waugh), and Italian Ministry of University and Scientific Research 2003 (R. Montironi).

The costs of publication of this article were defrayed in part by the payment of page charges. This article must therefore be hereby marked *advertisement* in accordance with 18 U.S.C. Section 1734 solely to indicate this fact.

Note: C. Murphy and M. McGurk contributed equally to this work.

Requests for reprints: David J.J. Waugh, Centre for Cancer Research and Cell Biology, Queens University Belfast, University Floor, Belfast City Hospital, Lisburn Road, Belfast BT9 7AB, Northern Ireland. Phone: 44-2890-263911; Fax: 44-2890-263744; E-mail: d.waugh@qub.ac.uk.

Materials and Methods

Chemicals and reagents. All chemicals were sourced from the Sigma Chemical Co. (St. Louis, MO) unless otherwise stated.

Cells and cell culture. PC3 human prostate adenocarcinoma cells were purchased from the American Type Culture Collection (Manassas, VA) and were maintained in RPMI 1640 supplemented with 10% fetal bovine serum and 2 mmol/L L-glutamine (Life Technologies, Paisley, United Kingdom). PC3-CXCR2.1 cells were developed by stable transfection of PC3 cells with a pcDNA3.1/V5.His.TOPO expression plasmid containing the coding sequence of the human CXCR2 receptor to maintain stable expression of this receptor in cell culture. CXCR2-expressing clones were determined and selected using reverse transcription-PCR and immunoprecipitation-immunoblotting analysis.[3] All cells were maintained in a humidified atmosphere of 5% CO_2 at 37°C.

Prostate biopsy tissues. The study used biopsy tissues from 40 patients (mean age, 67 years) with androgen-dependent prostate cancer. Three criteria were adopted in the selection of the biopsies: length of the core is 1.5 cm, 50% of each core occupied by cancer, and absence of acute and chronic inflammation. The Gleason score was 6 in 14 patients (all with clinical T_2 prostate cancer and total prostate-specific antigen serum level ≤4.00 ng/mL), 7 in 12 patients (5 patients were 3 + 4 and 7 patients were 4 + 3; all with clinical T_3 prostate cancer and total prostate-specific antigen serum level ≤10.00 ng/mL), and 8 to 10 in 14 patients (7 patients were 4 + 4, 3 patients were 4 + 5, and 4 patients were 5 + 5; all with clinical T_3 prostate cancer and total prostate-specific antigen serum level ≥10.00 ng/mL). High-grade prostatic intraepithelial neoplastic (PIN), the direct precursor of prostate cancer, was present in 10 cases. The study also included transurethral resection of the prostate material from 10 patients (mean age, 77 years) with androgen-independent prostate cancer. In these patients, progression was defined as at least two consecutive increases in prostate-specific antigen, obtained at least 2 weeks apart, in the presence of castrate levels of testosterone. The numbers of tissues studied for each of the conditions examined are shown in Table 1. All material was retrieved from the files of the Section of Pathological Anatomy and Histopathology, Polytechnic University of the Marche Region (Ancona) and was used according to the appropriate ethical guidelines.

Immunohistochemistry. Six consecutive 4 μm thick sections were cut from paraffin-embedded tissue blocks and prepared for immunohistochemistry as described previously (7). Tissue sections were incubated for 2 hours with the following monoclonal mouse antibodies diluted in 10% normal horse serum and 0.05% Tween 20: anti-IL-8 (1:500; Serotec, Kidlington, United Kingdom), anti-CXCR1 (1:500; Biosource, Camarillo, CA), anti-CXCR2 (1:500; Biosource), anti-Ki-67 (MIB1; 1:250; AMAC, Inc., Westbrook, ME), anti-CD34 (1:50), and anti–cyclin D1 (Novocastra Laboratories Ltd., Newcastle, United Kingdom). Immunoreactivity was detected using a secondary biotinylated horse anti-mouse antibody diluted 1:200 in 10% normal horse serum with 0.05% Tween 20. Following inhibition of endogenous peroxidase activity by treatment with 3% hydrogen peroxide in CMF/PBS and sodium azide for 30 minutes, the peroxidase reaction was developed for 5 minutes with 3,3′-diaminobenzidine tetrahydrochloride medium. Slides were counterstained with hematoxylin, washed, dehydrated in graded ethanol solutions and xylene, mounted with Permount (Fischer Scientific Co., Fair Lawn, NJ), and coverslipped. Appropriate positive and negative controls were obtained by concurrently staining cases known to express each antigen and by substituting the primary antibody with PBS, respectively.

Immunohistologic evaluation. A total of 1,000 tumor cells were counted in contiguous ×400 microscopic fields. IL-8, CXCR1, and CXCR2 expression in biopsy and transurethral resection of the prostate material was analyzed with regard to expression within the cytoplasm or staining localized to the apical and nonapical aspects of the cell membrane ("apical" refers to staining present in the luminal border of the cells and "nonapical" refers to staining localized to the membrane at the base of the cells, toward the stroma, opposite to the apical border, and in the lateral aspects of the cell membrane). Due to the absence of lumina in Gleason pattern 5 and/or androgen-independent cancer, membranous staining in these tumors was classified as a circumferential distribution. The number of cells demonstrating positive staining was expressed as the percentage of total cells counted. Similarly, positively staining cells in normal prostate tissue and high-grade PIN were first identified under scanning, low-power magnification, and contiguous fields were studied until a total of 1,000 benign, epithelial cells were counted. All scoring was conducted in a blinded fashion by a trained pathologist (R.M.).

Table 1. Numbers of tissues examined for each of the conditions studied

	No. tissues
Normal prostate	40
High-grade PIN	10
Prostate cancer, Gleason pattern 3	40
Prostate cancer, Gleason pattern 4	33
Prostate cancer, Gleason pattern 5	7
Androgen-independent prostate cancer	10

To measure Ki-67 expression in normal prostate tissue, high-grade PIN, and cancer, areas showing the highest density of proliferating epithelial cells identified by brown nuclear staining on low-power magnification were selected. A total of 1,000 tumor cell nuclei were counted in contiguous ×400 microscopic fields and the number of positively stained cells was expressed as the percentage of total cells counted. Microvessel density (MVD) within invasive tumor, high-grade PIN, or adjacent normal tissue was determined using the criteria of Weidner et al. (8). Using an Olympus BH-2 microscope (Tokyo, Japan), MVD was measured in microvessel "hotspots" corresponding to areas containing the highest density of microvessels. Using a ×20 objective and ×10 ocular, MVD was the total number of microvessels found in a 0.720 mm^2 area.

Data were collected and reported separately for the primary and secondary Gleason patterns or grades. When values are reported, for instance, for cancer Gleason pattern 3, we refer to all areas with such a pattern, independently of whether primary or secondary.

Immunocytochemistry. Cells were grown on coverslips for 24 hours, washed twice in PBS, fixed in acetone, and treated with one or more of the following primary antibodies at the indicated dilution: anti-CXCR1 mouse monoclonal (1:1,000, Biosource) or anti-CXCR2 mouse monoclonal (1:1,000, Biosource). Immunoreactivity for the receptors was developed using a 1:40 dilution of TRITC-conjugated goat anti-mouse IgG secondary antibody (Sigma Chemical). Colocalization with transferrin was conducted by incubation with anti-transferrin rabbit polyclonal (1:400, DAKO, Ely, United Kingdom) followed by FITC-conjugated swine anti-rabbit secondary antibody (1:40, DAKO). Images were analyzed using a fluorescence microscope (Leica DMLB, Heerbrugg, Switzerland).

Western blotting. Cells were lysed in radioimmunoprecipitation assay buffer [10 mmol/L Tris-HCl (pH 7.4), 150 mmol/L NaCl, 1 mmol/L EDTA, 1% (w/v) Triton X-100, 0.1% SDS, 1 protease inhibitor tablet per 10 mL (Roche Diagnostics, Inc., Lewes, United Kingdom), 100 nmol/L Na_3VO_4] and the lysates were cleared by centrifugation at 15,000 × *g* for 20 minutes at 4°C. Following electrophoresis and transfer, Hybond-P membranes were probed with anti-phospho-Thr^{202}/Tyr^{204} p44/p42 Erk kinase (1:1,000 dilution) and or anti-phospho-p38 mitogen-activated

[3] Pettigrew et al., in preparation.

protein kinase (MAPK) kinase (1:1,000 dilution; Cell Signaling Technology, Beverly, MA). Specific staining was detected using the chemiluminescence detection system (SuperSignal, Pierce, Rockford, IL).

ELISA. Cells (5×10^5 per well) were plated and incubated overnight under standard culture conditions. Cells were replenished and cultured in serum-free RPMI for 24 hours at which point medium was collected, and centrifuged at $1,000 \times g$ for 5 minutes to remove cell debris, and the supernatant was stored at −20°C until assayed. The cell number in each well was determined by parallel cell count analysis. The IL-8 concentration in each sample was calculated by comparison to a standard curve generated from a stock vial of IL-8 calibrated against the WHO interim international standard (1 WHO unit = 10 ng IL-8). Assays were conducted according to the manufacturer's instructions (Pelikrine Compact IL-8 ELISA kit, Beckman Coulter, High Wycombe, United Kingdom). Absorbance readings were taken at 450 nm using a microwell plate reader (Emax precision, Molecular Devices, Wokingham, United Kingdom).

Flow cytometry. Cells were trypsinized and resuspended in serum-free RPMI without phenol red at a density of 1×10^6 cells/mL. CXCR1 receptor expression was detected using a 1:100 dilution of anti-human CXCR1 monoclonal antibody (Serotec) against a 1:200 mouse IgG2b isotype-matched negative control antibody (DAKO). CXCR2 receptor expression in cells was detected by incubation with a 1:200 dilution of anti-human CXCR2 monoclonal antibody (Biosource) against a 1:400 dilution of a mouse IgG1 isotype-matched negative control antibody (DAKO). All primary antibody incubations were conducted for 1 hour at 4°C. After three washes in serum-free RPMI phenol red–free medium, cells were incubated for 1 hour at 4°C with rabbit anti-mouse IgG secondary antibody labeled with FITC (1:40, DAKO). Cells were washed twice in serum-free RPMI, resuspended in PBS plus 0.05% bovine serum albumin, and analyzed for surface expression on the flow cytometer (Becton Dickinson, Oxford, United Kingdom). For the analysis of total receptor expression of CXCR1 or CXCR2, cells were washed once in PBS plus 0.05% bovine serum albumin and then in PBS plus 0.05% bovine serum albumin containing 10% (v/v) FCS. Cells were fixed for 90 seconds in BFA [16 μL PBS, 330 μL (33%, v/v) formaldehyde, 600 μL acetone, 450 μL H_2O] and washed twice in saponin buffer (50 mmol/L D-glucose, 1 μg/mL saponin) before incubation with the primary antibody. Cells were subsequently treated as for determination of cell surface receptor expression, except that all incubations and washes were conducted in saponin buffer.

Cell count proliferation assay. Cells were seeded in 24-well plates at a density of 1×10^5 per well overnight in serum-free RPMI (2 mL). Fresh RPMI (1 mL) was added to each well, following which recombinant human IL-8 (rh-IL-8; Sigma Chemical), neutralizing antisera, or small-molecule antagonists were added. Cells were incubated at 37°C in a humidified 5% CO_2 atmosphere for 72 hours, trypsinized, and counted in triplicate using a Coulter Z Series particle count and size analyzer (Beckman Coulter) at threshold values of T_U 21 and T_L 5. Cell numbers were normalized to control values and statistical analysis of the data was done using GraphPad Prism 3.0 software.

Electroporation of PC3 cells. Cells were trypsinized and then centrifuged at $2,300 \times g$ for 5 minutes at 4°C. Cells were resuspended in a minimal volume of medium, incubated on ice for 5 minutes, and transferred into electrophoretic cuvettes. Antisera and antagonists were added to the medium at the appropriate concentration following which the cuvette was pulsed at 2.4 V on a gene pulser (Bio-Rad, Hemel Hempstead, United Kingdom) for 5 seconds. Cells were placed immediately on ice for a further 5 minutes, following which cells were seeded into appropriate tissue culture dishes. To account for any nonspecific effects of electroporation, control cell populations were electroporated in medium alone containing no antibody or inhibitor.

Statistical analysis. For immunohistochemistry data, statistical analysis was done with SPSS 9.0 software. Data derived from the primary and secondary Gleason 3 pattern as well as from the pattern 4 were considered separately and not as a single score. The significance of the observed differences was evaluated with the Mann-Whitney test, whereas the correlation between different features was calculated by applying the Pearson test. Differences observed in cell proliferation assays between the control and treated groups were analyzed for statistical significance using a two-tailed Student's t test comparison (GraphPad Prism).

Results

Interleukin-8 expression in prostate biopsy tissue with prostate cancer of Gleason pattern 3 and/or 4—Apical expression. In normal prostate, weak to moderate expression of IL-8 was localized to the apical or luminal border of the secretory cells (Table 2). The proportion of cells demonstrating an apical pattern of expression ranged from 50% to 100% (mean ± SD, 82.0 ± 12.44%). In comparison, the proportion of cancer cells (Gleason pattern 3 and 4) exhibiting apical staining for IL-8 was considerably lower than normal epithelium, ranging from 10% to 90% (mean, 57.33 ± 17.6%; $P < 0.001$). Apical IL-8 expression in high-grade PIN was intermediate between that observed in cancer and normal epithelium (72.5 ± 9.57%; range, 60-80%), reaching statistical significance from that detected on cancer cells ($P = 0.0047$) but not from the expression pattern on normal epithelium. There was no statistically significant difference in the proportion of cancer cells exhibiting IL-8 expression on their apical border when comparing Gleason 3 pattern against Gleason pattern 4 or when comparing primary against secondary Gleason pattern 3 regions.

Table 2. Distribution of IL-8 staining in prostate tissue [mean ± SD (range), %]

	Apical	Nonapical	Circumferential	Cytoplasm
Normal prostate	82.0 ± 12.44 (50-100)	0	0	0
High-grade PIN	72.5 ± 9.57 (60-80)	5.00 ± 10 (0-20)	1.00 ± 0.3 (0-1.5)	17.5 ± 9.57 (10-30)
Prostate cancer, Gleason pattern 3	61.13 ± 15.67 (20-90)	30.21 ± 9.92 (10-50)	3.2 ± 1.1 (1-4)	20.25 ± 10.00 (10-50)
Prostate cancer, Gleason pattern 4	52.73 ± 18.92 (0-70)	34.87 ± 18.13 (0-70)	6.3 ± 4.3 (2-9)	30.48 ± 9.06 (10-50)
Prostate cancer, Gleason pattern 5	NA	NA	47.00 ± 7.89 (40-60)	46.00 ± 5.77 (35-55)
Androgen-independent prostate cancer	NA	NA	52.86 ± 7.56 (40-60)	53.00 ± 9.66 (40-70)

NOTE: See text for the results of statistical analysis. NA, not applicable.

Nonapical expression. In contrast to normal prostate epithelial cells, we detected a nonapical pattern of membranous IL-8 expression in cancer cells (Fig. 1A). The proportion of cancer cells exhibiting a nonapical membrane expression of IL-8 ranged from 5% to 70% (mean, 32.65 ± 14.96%). This nonapical pattern expression of IL-8 was also present in all 10 cases of high-grade PIN studied, but the mean number of positive cells was much lower (i.e., 5.0 ± 10%; range, 0-20% of cells). Although the absence of IL-8 staining with a nonapical pattern in normal epithelial cells prohibited quantitative statistical analysis, the difference observed in nonapical pattern expression between cancer cells and those cells within foci of high-grade PIN was statistically significant (P = 0.001). Again, the differences observed in cell membrane expression of the nonapical pattern between Gleason 3 and 4 and between primary and secondary Gleason pattern 3 were not statistically significant. A small proportion of cells in high-grade PIN and in Gleason pattern 3 and 4 cancer showed a circumferential pattern of staining (Table 2).

Cytoplasmic expression. The number of cancer cells exhibiting cytoplasmic expression of IL-8 ranged from 10% to 50% (mean, 23.97 ± 10.37%; Fig. 1A). Cytoplasmic expression of IL-8 was also detected in high-grade PIN. The number of positive cells ranged from 10% to 30% (mean, 17.5 ± 9.57%) and was not statistically different from the cytoplasmic IL-8 expression observed in adjacent cancer cells. Cytoplasmic IL-8 staining was not observed in normal prostate epithelial cells. There were no statistically significant differences observed in comparing the profile of cytoplasmic IL-8 expression between primary and secondary Gleason pattern 3 within the biopsy sections. However, the difference between Gleason 3 and 4

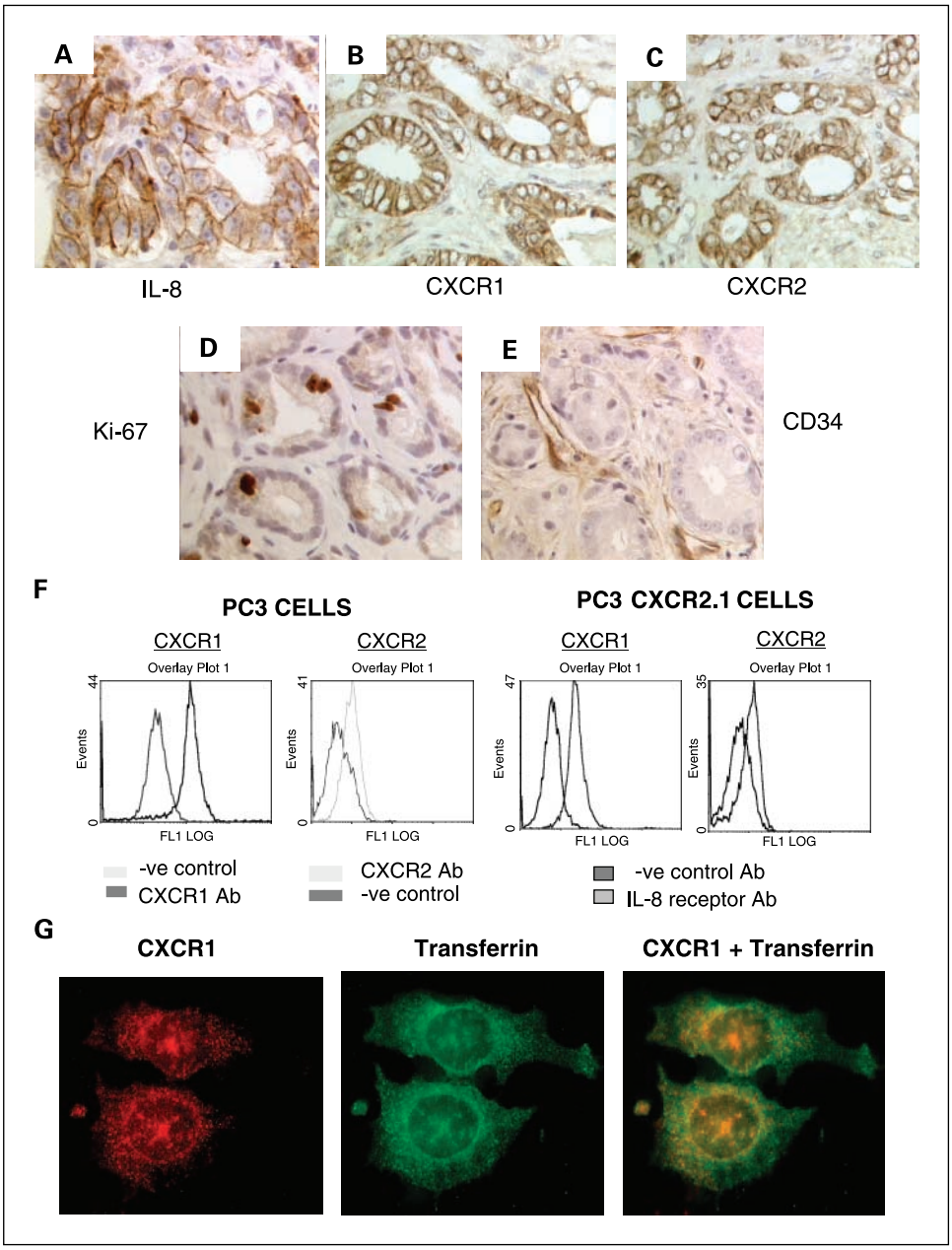

Fig. 1. Characterization of IL-8, CXCR1, and CXCR2 expression in human prostate biopsy and/or androgen-independent cancer cells. *A*, staining for IL-8 in a T_2, Gleason pattern 4 biopsy specimen. Immunoreactivity to the IL-8 antibody is present both in the apical and basal aspects of the membrane and in the cytoplasm of cancer cells. *B*, staining for CXCR1 in a T_2, Gleason pattern 3 biopsy specimen. *C*, staining for CXCR2 in a T_2, Gleason pattern 3 biopsy specimen. Immunoreactivity to each of these IL-8 receptors was detected within the cytoplasmic compartment of cells in addition to the apical and basal aspects of the cell membrane. *D*, expression of the cell proliferation marker Ki-67 in cancer cells of a T_2, Gleason pattern 3 biopsy section. *E*, staining of CD34 to analyze MVD in a T_2, Gleason pattern 3 biopsy section. Staining for each of these antigens (*A*-*E*) was developed using an indirect immunoperoxidase protocol as described in Materials and Methods. *F*, characterization of CXCR1 and CXCR2 distribution in saponin-permeabilized androgen-independent PC3 and PC3-CXCR2.1 cells using flow cytometry analysis. Strong expression of each receptor was detected by incubating cells for 1 hour with monoclonal antibodies raised against human CXCR1 and CXCR2, respectively. The intensity of fluorescence detected in all flow cytometry is compared with the appropriate negative controls. Parallel experiments on nonpermeabilized cells indicated minimal cell surface expression of CXCR1 and CXCR2 receptors on both PC3 and PC3-CXCR2.1 cells, therefore suggesting a predominant intracellular expression of both CXCR1 and CXCR2 receptors in these cells. *G*, intracellular localization of CXCR1 receptors in the cytoplasm of PC3 cells as shown by immunocytochemistry. Cells were fixed and then incubated with either a monoclonal antibody to human CXCR1 or transferrin. Immunostaining for human CXCR1 was detected using a TRITC-labeled secondary antibody, whereas specific transferrin immunoreactivity was detected using a FITC-labeled secondary antibody.

Table 3. Distribution of CXCR1 staining in prostate tissue [mean ± SD (range), %]

	Apical	Nonapical	Circumferential	Cytoplasm
Normal prostate	79.5 ± 8.97 (60-100)	0.25 ± 1.58 (0-10)	0	0.62 ± 2.32 (0-10)
High-grade PIN	70.0 ± 0 (70-70)	5.0 ± 10 (0-20)	0.90 ± 0.40 (0.4-1.5)	22.50 ± 6.45 (15-30)
Prostate cancer, Gleason pattern 3	61.63 ± 10.71 (40-80)	30.50 ± 11.70 (10-60)	3.30 ± 1.80 (0.7-5.0)	17.62 ± 6.20 (10-30)
Prostate cancer, Gleason pattern 4	56.36 ± 6.88 (45-70)	31.36 ± 7.10 (15-50)	6.5 ± 3.0 (2.5-9.0)	27.12 ± 7.29 (15-45)
Prostate cancer, Gleason pattern 5	NA	NA	52.14 ± 7.56 (45-65)	47.86 ± 4.88 (40-55)
Androgen-independent prostate cancer	NA	NA	50 ± 6.24 (40-60)	54 ± 5.68 (45-60)

NOTE: See text for the results of the statistical analysis.

pattern was statistically significant ($P < 0.001$). Statistical analysis revealed the presence of correlation between nonapical membrane expression of IL-8 and cytoplasmic expression of IL-8 in cancer cells ($R = 0.26$; $P = 0.025$).

Interleukin-8 receptor expression in prostate biopsy tissue with prostate cancer of Gleason pattern 3 and/or 4. Analysis revealed a strong correlation between the expression profile observed for IL-8 and the expression of its receptor CXCR1 ($R = 0.82$; $P < 0.001$). As seen with IL-8, the expression of CXCR1 on the apical border decreases significantly on progression from normal prostate secretory cells (79.50 ± 8.79%) to high-grade PIN (70 ± 15.11%) and cancer (59.25 ± 9.49%), respectively (Table 3). CXCR1 expression showed a predominantly apical pattern of staining at the level of the cell membrane in normal prostate, whereas it became mostly nonapical and cytoplasmic in cancer cells (Fig. 1B). Nonapical membrane staining for CXCR1 was absent in normal prostate secretory epithelium but was detectable in high-grade PIN and was increasingly present in cancer cells in correlation with increasing Gleason score. Similarly, the expression of CXCR1 in the cytoplasm of normal prostate epithelial cells, high-grade PIN, and cancer cells was 0%, 22.50 ± 6.45%, and 21.92 ± 8.19%, respectively. The expression profile and distribution of the other human IL-8 receptor CXCR2 in the prostate biopsy tissues was similar to that observed for CXCR1 and is detailed in Table 4 (see also Fig. 1C). For instance, when compared with CXCR1 localization, there was a high correlation to the loss of CXCR2 expression on the apical membrane ($R = 0.83$; $P < 0.001$).

In addition to identifying the altered distribution of both the ligand and its receptors, the intensity of IL-8, CXCR1, and CXCR2 staining in cancer cells and high-grade PIN was predominantly moderate to strong (++/+++) as opposed to weaker expression (+) in neighboring normal prostate tissue. The basal cells present in normal prostate and in high-grade PIN did not show appreciable staining for IL-8, CXCR1, and CXCR2.

Correlation of interleukin-8 expression with cell proliferation (Ki-67) in prostate biopsy tissue with prostate cancer of Gleason pattern 3 and/or 4. The percentage of proliferating tumor cells (Ki-67-positive cells) with Gleason pattern 3 and 4 ranged from 2.0% to 16.00% (mean, 8.05 ± 3.63%; Fig. 1D). Ki-67-positive cells in neighboring normal prostate tissue were less conspicuous and appeared to be predominately in basal cells by location, whereas the incidence of proliferating cells in high-grade PIN was similar to that observed in cancer cells (Table 5). As expected, the differences between cancer and normal and between high-grade PIN and normal were statistically significant ($P < 0.001$ and $P < 0.001$, respectively), but there was no difference between cancer and high-grade PIN. Furthermore, a significant difference in proliferating cells was observed between Gleason pattern 3 (mean, 5.16 ± 1.5%) and Gleason pattern 4 (mean, 11.56 ± 1.96%; $P < 0.001$). The difference between primary and secondary Gleason pattern 3 was not statistically significant.

Significantly, Ki-67 staining was inversely correlated with the expression of IL-8 on the apical or luminal border of cells ($R = -0.6$; $P < 0.001$). In contrast, there was a direct correlation of nonapical pattern of the cell membrane ($R = 0.67$; $P < 0.001$) and cytoplasmic IL8 expression ($R = 0.79$; $P < 0.001$) with this cell proliferation marker. Similar positive correlations were also observed between cell proliferation and (*a*) nonapical membrane expression of each of the IL-8 receptors and (*b*) cytoplasmic expression of these receptors in cancer cells (data not shown).

Table 4. Distribution of CXCR2 staining in prostate tissue [mean ± SD (range), %]

	Apical	Nonapical	Circumferential	Cytoplasm
Normal prostate	79.88 ± 6.84 (70-95)	0	0	0.13 ± 0.79 (0-5)
High-grade PIN	71.25 ± 2.50 (70-75)	13.75 ± 9.46 (0-20)	1.50 ± 0.50 (0.5-2.5)	16.25 ± 4.79 (10-20)
Prostate cancer, Gleason pattern 3	64.50 ± 7.91 (50-80)	29.25 ± 9.17 (15-50)	3.50 ± 1.20 (0.8-4.8)	16.75 ± 4.74 (5-25)
Prostate cancer, Gleason pattern 4	54.85 ± 7.34 (35-70)	33.18 ± 5.84 (20-45)	6.8 ± 3.9 (2.1-9.2)	28.94 ± 5.27 (20-40)
Prostate cancer, Gleason pattern 5	NA	NA	48.57 ± 7.48 (40-70)	47.86 ± 2.67 (45-50)
Androgen-independent prostate cancer	NA	NA	47 ± 8.88 (35-60)	56.50 ± 5.80 (45-65)

NOTE: See text for the results of the statistical analysis.

Table 5. Cell proliferation, cyclin D1 expression, and MVD [mean ± SD (range), %]

	Ki-67	Cyclin D1	MVD
Normal prostate	0.56 ± 0.30 (0.1-1.2)	2.53 ± 1.30 (0.8-5)	35.42 ± 9.62 (19-51)
High-grade PIN	5.92 ± 1.28 (4.5-7.19)	13.00 ± 2.94 (9-16)	60.75 ± 5.97 (52-65)
Prostate cancer, Gleason pattern 3	5.16 ± 1.50 (2-8.4)	11.57 ± 2.96 (6-18)	66.85 ± 7.61 (50-80)
Prostate cancer, Gleason pattern 4	11.56 ± 1.96 (8.3-16)	18.67 ± 2.31 (15-24)	103.06 ± 13.50 (70-126)
Prostate cancer, Gleason pattern 5	19.86 ± 1.93 (17-22)	23.86 ± 1.77 (21-26)	138.86 ± 6.41 (129-150)
Androgen-independent prostate cancer	24.70 ± 4.40 (20-35)	26.70 ± 2.83 (21-30)	154.20 ± 17.51 (135-190)

NOTE: See text for the results of statistical analysis.

Correlation of interleukin-8 expression with cyclin D1 in prostate biopsy tissue with prostate cancer of Gleason pattern 3 and/or 4. Expression of cyclin D1 was detected in cells of high-grade PIN (range, 9-16%) and in tumor cells (range, 6-24%; Table 5). In contrast, cyclin D1–positive cells in neighboring normal prostate tissue were less conspicuous and appeared to be predominately located within the basal cell layer. The differences in cyclin D1 expression observed between cancer cells and normal and between high-grade PIN and normal were statistically significant ($P < 0.001$ and $P < 0.001$, respectively), but there was no statistical significance between cyclin D1 expression observed in cancer cells and those in foci of high-grade PIN. When considering cyclin D1 expression in the two Gleason patterns, a significant difference was present between Gleason 3 pattern (mean, 11.57 ± 2.96%) and Gleason 4 pattern (mean, 18.67 ± 2.31%; $P < 0.001$). As expected, there was a positive correlation between cell proliferation (Ki-67 expression) and cyclin D1 expression ($R = 0.89$; $P < 0.001$).

Cyclin D1 expression was positively correlated with the nonapical membrane expression of IL-8 and cytoplasm IL-8 expression (nonapical: $R = 0.71$; $P < 0.001$; cytoplasmic: $R = 0.79$; $P < 0.001$). Similarly, the expression of CXCR1 and CXCR2 to the nonapical aspect of the membrane and to the cytoplasm also correlated with cyclin D1 expression (CXCR1, nonapical: $R = 0.71$; $P < 0.001$; cytoplasmic: $R = 0.83$; $P < 0.001$; CXCR2, nonapical: $R = 0.79$; $P < 0.001$; cytoplasmic: $R = 0.87$; $P < 0.001$).

Correlation of interleukin-8 expression with microvessel density in prostate biopsy tissue with prostate cancer of Gleason pattern 3 and/or 4. The intratumoral MVDs for prostate carcinomas ranged from 50 to 126 (mean, 83.22 ± 21.02; Table 5; Fig. 1E). For the adjacent normal prostate tissue, MVD ranged from 19 to 51 (mean, 35.42 ± 9.62), whereas MVD in high-grade PIN was intermediate to that observed in regions of cancer and histologically normal prostate tissue ranging from 50 to 65 (mean, 60.75 ± 5.97). The observed differences in MVD between prostate cancer and normal prostate tissue and between high-grade PIN and normal prostate tissue were each statistically significant ($P < 0.001$ and $P < 0.001$, respectively). The difference between cancer and high-grade PIN was also statistically significant ($P = 0.009$). MVD was significantly higher in Gleason pattern 4 cancers when compared with Gleason pattern 3 (Table 5; $P < 0.001$), but no difference between primary and secondary Gleason pattern 3 was detected in our study. MVD was directly correlated with the nonapical pattern ($R = 0.73$; $P < 0.001$) and cytoplasmic expression ($R = 0.81$; $P < 0.001$) of IL-8 and inversely correlated with the apical or luminal border expression ($R = -0.57$; $P < 0.001$). Furthermore, there was a strong correlation between MVD and that of cell proliferation ($R = 0.88$; $P < 0.001$).

Interleukin-8, CXCR1, CXCR2, Ki-67, cyclin D1, and microvessel density in Gleason pattern 5 prostate cancer and in androgen-independent prostate cancer. IL-8, CXCR1, and CXCR2 expression in androgen-dependent prostate cancer with Gleason grade 5 was principally characterized by a circumferential pattern of cell membrane and cytoplasmic staining (Table 2). Relative to the nonapical and circumferential expression pattern of IL-8 expression in Gleason pattern 3 and 4, there was a statistically significant increase in the numbers of cells exhibiting circumferential IL-8 expression in Gleason pattern 5 (47.0 ± 7.89%; $P < 0.001$). Similarly, cytoplasmic IL-8 expression was also more marked than that observed in cancers with Gleason pattern 3 and 4 (46.00 ± 5.77%; $P = 0.001$; Table 2). As before, the distribution of CXCR1 and CXCR2 expression correlated to that observed for IL-8, with statistically significant increases in cytoplasmic expression in Gleason pattern 5 cancers when compared with Gleason pattern 3 and 4 tumors ($P < 0.001$ and $P < 0.001$, respectively; Tables 3 and 4). Gleason grade 5 cancer was also associated with a higher degree of proliferation, a greater cyclin D1 expression, and an increased MVD in comparison with Gleason 3 and 4 cancer (Table 5).

Qualitatively, the IL-8 and IL-8 receptor expression pattern in androgen-independent prostate cancer was similar to that observed in Gleason grade 5 cancer (Tables 2, 3, and 4), with strong circumferential and cytoplasmic expression detected in cancer cells. There was a statistically significant increase in the proportion of cells exhibiting cytoplasmic expression of IL-8 in androgen-independent cancer ($P < 0.001$) relative to that detected in Gleason pattern 3 or 4 (Table 2). CXCR1 and CXCR2 expression correlated with that of IL-8, with strong expression detectable in the cytoplasm of cancer cells (Tables 3 and 4). Ki-67, cyclin D1 expression, and MVD in androgen-independent prostate cancer were higher than in Gleason grade 5 cancer (Table 2), with each of these differences attaining statistical significance (Ki-67, $P = 0.005$; cyclin D1, $P = 0.03$; MVD, $P = 0.04$).

Characterization of interleukin-8, CXCR1, and CXCR2 expression in androgen-independent prostate cancer PC3 cells. We conducted *in vitro* experiments on the androgen-independent PC3 cell line to provide further experimental evidence to support the correlation of IL-8 expression with cell proliferation. Consistent with the elevated IL-8 expression in

androgen-independent disease *in vivo*, we detected constitutive IL-8 expression in parental PC3 cells by immunoblotting (data not shown) and secretion of IL-8 from PC3 cells into the cell culture medium by ELISA. In addition, we selected a clonal derivative of PC3 cells, PC3-CXCR2.1, which exhibited stable expression of the CXCR2.1 receptor (2-fold increase over parental empty vector–transfected PC3 cells by immunoblotting; data not shown) and elevated expression of IL-8 relative to parental cells. The level of IL-8 secreted by the PC3-CXCR2.1 cells (44.8 ± 2.3 ng/mL/10^6 cells/24 hours; $n = 4$) was significantly higher than that detected in PC3 cells (1.35 ± 0.16 ng/mL/10^6 cells/24 hours; $n = 4$). The expression of CXCR1 and CXCR2 receptors on PC3 and PC3-CXCR2.1 cells was shown by immunoprecipitation-Western blotting (data not shown) and flow cytometry using the same antibodies employed to detect CXCR1 and CXCR2 receptors *in vivo*. Abundant CXCR1 expression but weak CXCR2 expression were detected on the cell surface of the parental PC3 cells (data not shown). Conversely, negligible expression of either CXCR1 or CXCR2 was detected on the surface of the PC3-CXCR2.1 cells by flow cytometry (data not shown). Expression of these receptors within the cytoplasm of either cell was subsequently determined by repeating the flow cytometry analysis on saponin-permeabilized cells. Large shifts in fluorescence intensity were detected in PC3 cells following incubation with anti-CXCR1 antibodies, whereas modest shifts in fluorescence were observed following incubation with anti-CXCR2 antibodies (Fig. 1F, *left*). A similar profile of CXCR1 and CXCR2 expression on PC3-CXCR2.1 cells was also detected in this analysis (Fig. 1F, *right*). The profile of receptor expression and distribution detected for each of the CXCR1 and CXCR2 receptors on PC3 cells was confirmed by further flow cytometry experiments using anti-CXCR1 and anti-CXCR2 monoclonal and polyclonal antibodies obtained from three other commercial sources (data not shown). In addition to confirming the membranous and cytoplasmic distribution of these receptors in PC3 cells *in vitro*, these flow cytometry and immunoblotting results confirm the specificity of the antibodies used to detect CXCR1 and CXCR2 expression on human prostate biopsy sections. Furthermore, consistent with our observations *in vivo*, flow cytometry analysis suggests that IL-8 receptors are predominately localized to the cytoplasm in androgen-independent prostate cancer cells, because parallel studies on DU145 cells yielded similar results (data not shown). Finally, cell surface and intracellular distribution of IL-8 receptors in each of the cell lines was confirmed by immunocytochemistry. As shown for CXCR1 expression in parental PC3 cells (Fig. 1G), we detected receptor distribution on the plasma membrane, throughout the cytoplasm, and a concentrated localization of the receptors in the perinuclear space. There was a strong correlation between the perinuclear distribution of CXCR1 and CXCR2 and the endosomal marker transferrin, suggesting that the prevalent intracellular distribution of IL-8 receptors detected in the prostate cancer cell lines may result from agonist-induced internalization of the receptor.

Interleukin-8 induces proliferation and activates mitogenic signaling pathways in PC3 cells. To determine whether IL-8 is a direct mitogen on prostate cancer cells, we examined the effect of stimulating PC3 or PC3-CXCR2.1 cells with exogenous rh-IL-8 on cell proliferation using cell count analysis. We observed concentration-dependent increases in the proliferation of PC3 cells in response to rh-IL-8 (Fig. 2A). The response was saturable at 10 nmol/L and increased the total cell number by 46% in the course of 72 hours over that of unstimulated cells. The apparent potency of the response was in the order of 1 nmol/L and correlates well with the known affinity of this ligand for each of its receptors. In addition, the potency of the mitogenic response was comparable with the potency of rh-IL-8 to stimulate the phosphorylation of p42/p44 Erk and p38 MAPK in PC3 cells (Fig. 2B).

In contrast, we observed no potentiation of PC3-CXCR2.1 cell proliferation in response to stimulation with rh-IL-8, suggesting that the level of constitutive IL-8 produced by this derivative cell line may be high enough to saturate the mitogenic response of these cells to this chemokine. To examine the significance of elevated constitutive IL-8 expression to PC3-CXCR2.1 cell proliferation, we used a series of pharmacologic approaches to abrogate endogenous IL-8 signaling. Cells were treated with an azide-free neutralizing antibody to IL-8, and the effect on cell proliferation was determined by cell count analysis following 72-hour exposure to this antibody. Unexpectedly, the addition of this antibody directly to the culture medium had no effect on cell proliferation (Fig. 3A). However, neutralizing the effect of cytoplasmic IL-8 by electroporating cells treated with the anti-IL-8 antibody resulted in a statistically significant 23.4 ± 4.8% decrease in PC3-CXCR2.1 cell number relative to control ($P < 0.01$; $n = 5$; Fig. 3A). Control cells were also subjected to electroporation and were shown to maintain proliferation over the course of experimentation. Furthermore, electroporation with isotype-matched antibodies had no effect on cell proliferation (data not shown). These experiments suggest that IL-8 retained within the cytoplasm of the cell is signaling competent and is sufficient to maintain and promote the proliferation of prostate cancer cells.

Interleukin-8 promotes cell proliferation through activation of CXCR1 and CXCR2 receptors. To determine whether either of the IL-8 receptors expressed in prostate cancer cells is selectively coupled to the promotion of cell proliferation, the individual contribution of CXCR1 and CXCR2 receptors to cell proliferation was studied using neutralizing antisera against each of the receptors. As seen with the anti-IL-8 antibody, cell surface targeting of either anti-CXCR1 or anti-CXCR2 antibodies had negligible effects on PC3-CXCR2.1 cell proliferation. However, electroporation of either antibody into PC3-CXCR2.1 cells attenuated cell proliferation (Fig. 3B); the anti-CXCR1 antibody (4 g/mL) reduced cell number by 18.2 ± 5.1% over the course of 72 hours ($P < 0.001$; $n = 3$), whereas similar treatment with an anti-CXCR2 antibody reduced the cell number by 19.7 ± 2.8% relative to control over 72 hours ($P < 0.001$; $n = 3$). Coelectroporation of anti-CXCR1 and anti-CXCR2 antibodies at these concentrations also decreased cell proliferation but did not produce an additive decrease in cell number relative to individual treatments (data not shown).

To verify the effects observed by targeting the IL-8 receptors with neutralizing antibodies, PC3-CXCR2.1 cells were also treated with the CXCR2-selective small-molecule inhibitor, SB225002. We administered this drug at a concentration of 8 nmol/L to confer selective abrogation of CXCR2 function. As shown, blockade of CXCR2 signal transduction using SB225002 reduced the cell number over 72 hours by 27.7 ± 3.2% relative to control ($P < 0.001$; $n = 3$; Fig. 3C), a response comparable with that observed with the anti-CXCR2 neutralizing antibody.

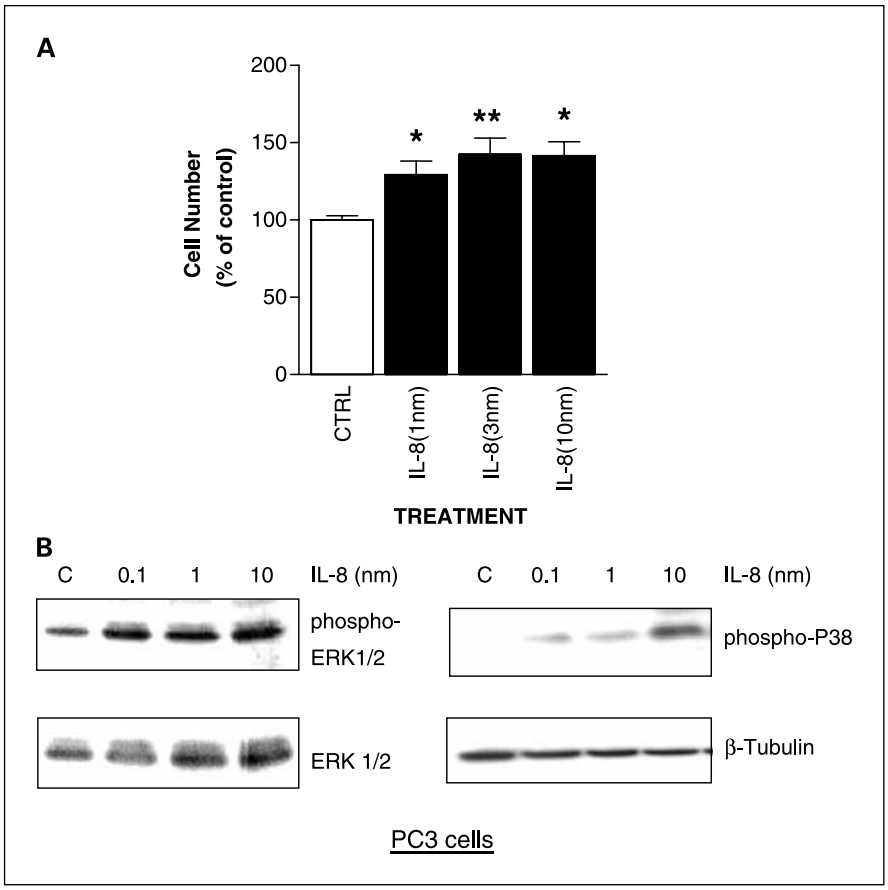

Fig. 2. Effect of exogenous IL-8 on PC3 cell proliferation and signaling. *A*, rh-IL-8 was added to PC3 cells and the effect on cell number over 72 hours was determined using cell count analysis. *Columns*, mean of three independent experiments, each done in triplicate; *bars*, SE. *, $P < 0.05$; **, $P < 0.01$. *B*, effect of rh-IL-8 in promoting the selective activation of MAPK signaling cascades in PC3 cells. Cells were treated with increasing concentrations of rh-IL-8 for 10 minutes. Protein lysates were then resolved by electrophoresis and probed with phosphorylation-specific antibodies to p42/p44 MAPK or p38 MAPK as described in Materials and Methods. Representative images of three independent experiments.

Discussion

Clinical and experimental studies associate the expression of the proinflammatory chemokine IL-8 with the metastasis and development of androgen independence of human prostate cancer (1–6). Despite this, our knowledge regarding the expression of IL-8 in both normal and neoplastic human prostate tissue is poorly understood. Therefore, immunohistochemistry was conducted on human prostate biopsy tissue to ascertain the expression of IL-8 and each of its receptors CXCR1 and CXCR2 in normal prostate epithelium and human prostate cancer cells. This study was conducted on a small but focused subset of biopsy samples that were representative of early-stage locally confined prostate cancer, locally invasive prostate cancer, and androgen-independent metastatic disease. As our study wished to determine cancer cell–related IL-8 and IL-8 receptor expression and effects, analysis was only conducted on those sections devoid of acute and chronic inflammation and neutrophil infiltrate that would otherwise negatively affect the ease of data interpretation.

Weak to moderate IL-8 expression was detectable on only the apical membrane of the majority of normal prostate epithelial cells. Moderate to strong expression of IL-8 was detected in prostate cancer cells; however, in marked contrast to normal epithelium, IL-8 expression not only was detectable on the apical membrane but also was found on the nonapical part of the membrane and within the cytoplasm of prostate cancer cells. The proportion of cells displaying nonapical and cytoplasmic expression of IL-8 progressively increased with stage of disease. Indeed, the observation of IL-8 immunoreactivity in the cytoplasm of cancer cells in prostate biopsy is consistent with the one previous study conducted (9). Our study also examined the expression of the two IL-8 receptors, CXCR1 and CXCR2, on normal prostate epithelial cells and in cancer cells. Again, expression of these receptors was strictly localized to the apical membrane of normal prostate epithelium. However, as with the expression of the ligand, each of the receptors was detected on the apical membrane, basal membrane, and within the cytoplasm of prostate cancer cells. Furthermore, the observed similarities and strong statistical correlations regarding the distribution of both ligand and receptor expression in prostate cancer cells would suggest that IL-8 may promote the disease progression of prostate cancer through increased autocrine/paracrine signaling responses.

Similar to our observations in cancer cells, IL-8 expression was detected within the cytoplasm of cells found within all foci of high-grade PIN. Similarly, CXCR1 and CXCR2 receptor expression was consistently detected within the cytoplasm of a subpopulation of cells in all PIN foci. These data indicate that the increased expression and altered distribution of IL-8, CXCR1, and CXCR2 expression observed in cancer cells is also apparent in high-grade PIN and suggests that IL-8 may have an important role to play in the molecular carcinogenesis of prostate cancer. Further studies regarding the expression of this CXC chemokine in more cases of PIN are merited to examine the significance of our observations.

Our data show a progressive increase in IL-8 expression in early-stage human prostate cancer (T_2, prostate-specific antigen

<4 ng/mL, Gleason 3 or 4) relative to normal prostate epithelium. In addition, the redistribution of IL-8 and IL-8 receptor expression to the cytoplasm and the basal membrane of prostate cancer cells was even more pronounced in the transurethral resection of the prostate samples of advanced and androgen-independent disease (Gleason pattern 5). These observations are consistent with the elevated expression of this chemokine previously detected in the serum of patients with prostate cancer, which reported 2- and 5-fold elevations in serum IL-8 levels in patients with localized prostate cancer or with metastatic disease, respectively, relative to normal or benign prostatic hypertrophy patients (5).

In animal models of prostate cancer, IL-8 was proposed to promote tumor growth as a secondary consequence of angiogenesis (1, 2, 10). Therefore, to determine whether IL-8 expression in human prostate cancer correlated with either angiogenesis or cell proliferation, the biopsy material was also scored for the expression of CD34, a marker of MVD, the cell proliferation marker Ki-67, and the cell cycle regulatory protein, cyclin D1. Cyclin D1 expression in prostate cancer is related to several malignant cellular features, including tumor-node-metastasis classification, histologic differentiation, perineural invasion, DNA ploidy, S-phase fraction, expression of Ki-67, and mitotic index (11) and bone metastasis (12). Consistent with the prior observations in orthotopic models of prostate cancer, our study showed a strong correlation between cell proliferation and MVD (1, 2, 9). Furthermore, we were able to show independent positive correlations between basal membrane and cytoplasmic expression of IL-8 and each of the IL-8 receptors to both cell proliferation and angiogenesis. Analysis also showed a negative correlation of apical expression of IL-8 and its receptors with both cell proliferation and angiogenesis. Therefore, our data clearly show that the altered distribution of IL-8 and its receptors in human prostate cancer at the primary anatomic site may play a significant role in progression of the disease.

Because IL-8 expression was highest in androgen-independent prostate cancer, we undertook a series of *in vitro* experiments in the androgen-independent PC3 cells to investigate the functional importance of IL-8 expression and signaling in advanced human prostate cancer. We used parental PC3 cells and a clonal derivative of the PC3 cells exhibiting high IL-8 expression because IL-8 has been reported previously to promote the tumorigenicity of this cell line (12). Characterization of PC3 cells confirmed constitutive expression and secretion of IL-8, whereas expression of both CXCR1 and CXCR2 receptors on these cells was confirmed by immunoprecipitation-Western immunoblotting (data not shown), flow cytometry, and immunocytochemistry. Similar to the results shown in prostate cancer cells *in vivo*, the CXCR1 and CXCR2 receptors were predominantly localized to the cytoplasm of these cells by flow cytometry and immunocytochemistry. The strong colocalization of these receptors with transferrin, an endosomal marker particularly in the perinuclear space, suggests that the intracellular distribution of IL-8 receptors may be

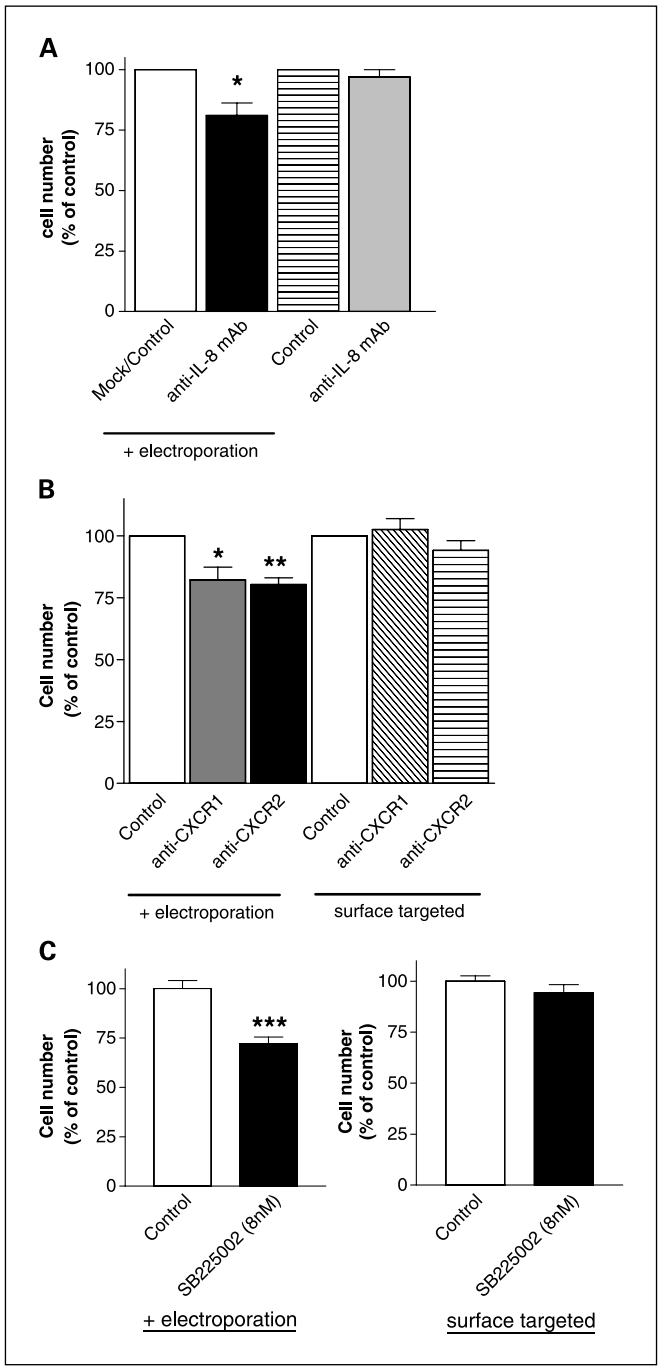

Fig. 3. Inhibition of constitutive IL-8 signaling attenuates the proliferation of PC3-CXCR2.1 cells. *A*, effect of a neutralizing anti-IL-8 antibody (4 μg/mL) on the proliferation of PC3-CXCR2.1 cells, given either directly to the cell culture medium or following electroporation into the cells. Cell number was shown to decrease when antibodies were targeted to IL-8 present within the cytoplasm of these androgen-independent prostate cancer cells. *Columns*, mean of five individual experiments; *bars*, SE. *B*, effect of neutralizing anti-CXCR1 antibody or neutralizing anti-CXCR2 antibody on PC3-CXCR2.1 cell proliferation. Antibodies were added directly to the cell culture medium or electroporated into the cells at a final concentration of 4 μg/mL. Similarly, antibodies attenuated cell proliferation when directed to the intracellular but not cell surface pool of IL-8 receptors. *Columns*, mean of three individual experiments; *bars*, SE. Treatment in either mode with isotype-matched antibodies had no effect on cell proliferation assays in either (*A*) or (*B*) above. *C*, effect of the CXCR2-selective small-molecule antagonist, SB225002, on the proliferation of PC3-CXCR2.1 cells. The compound was either electroporated into cells to target the intracellular CXCR2 receptor pool (*left*) or added to the cell culture medium to target the CXCR2 receptors expressed on the cell surface (*right*). *Columns*, mean of three individual experiments; *bars*, SE. *, $P < 0.05$; **, $P < 0.01$; ***, $P < 0.001$, statistically significant differences in cell number between untreated and treated cell populations (two-tailed Student's *t* test analysis).

related to agonist-induced internalization of the receptors (13, 14). Studies of IL-8 receptor turnover on the cell surface of neutrophils have reported that CXCR2 receptors are internalized at a faster rate and reexpressed on the cell surface at a slower rate than CXCR1 receptors (14). This may explain the ability to detect CXCR1 expression but not that of CXCR2 receptors on the cell surface of PC3 cells using these techniques. Alternatively, our observations are consistent with the prior localization of the nonglycosylated 40-kDa CXCR2 receptor (the single band identified in our immunoblotting experiments on PC3 cells) to the intracellular compartments of neutrophils and suggest that the strong localization of the CXCR2 receptor in the cytoplasm of prostate cancer cells *in vitro* and *in vivo* may result from decreased glycosylation of this receptor (15).

Prostate cancer cell lines exhibited constitutive expression of IL-8 together with expression of both IL-8 receptors, raising the possibility of autocrine signaling and responses in these cells. Consistent with the correlation of IL-8 expression in cancer cells to indices of cell proliferation in human prostate biopsy, prior studies have promoted the idea that IL-8 may function as an autocrine growth factor in pancreatic (16), ovarian (17, 18), and colon (19, 20) cancers. The correlation between IL-8 expression and cell proliferation was reaffirmed *in vitro* where increases or decreases were observed following either addition or removal of the IL-8 stimulus: the stimulation of PC3 cells, but not PC3-CXCR2.1 cells, with rh-IL-8 resulted in a concentration-dependent statistically significant increase in cell number, whereas the suppression of IL-8 signaling by antibodies attenuated the proliferation of the PC3-CXCR2.1 cells. Consistent with *in vivo* correlations, activation of both CXCR1 and CXCR2 receptors contribute to cell proliferation *in vitro*, suggesting the downstream signaling pathways activated by these receptors cooperate to promote cell cycle progression.

Stimulation of PC3 cells with rh-IL-8 at similar concentrations promoting proliferation induced a potent phosphorylation of p42/p44 Erk1/2 MAPK and p38 MAPK, correlating with the previously reported role of the Erk1/2 MAPK cascade in underpinning the mitogenic response of ovarian cancer cells to IL-8 (17). Other studies have confirmed elevated phosphorylation of each of these MAPKs in prostate cancer. Elevated phosphorylation of Erk1/2 has been observed in proliferating prostatic epithelial cells and has been associated with the initiation of prostate cancer (21). Phosphorylation and activation of p38 MAPK was increased in well-differentiated prostate tumors compared with normal prostate epithelial cells, whereas cells within PIN lesions expressing activated p38 MAPK were observed to be proliferative rather than apoptotic. Further experiments will be required to examine the role of each of these signaling pathways in the molecular mechanism underpinning IL-8 promoted proliferation of prostate cancer cells.

Prior studies discounted the role of IL-8 as a mitogenic factor in prostate cancer (1, 12), proposing instead that the tumorigenic action of IL-8 occurred as a secondary consequence of the proangiogenic activity of IL-8. Our current data show that the basal and cytoplasmic expression of IL-8 in human prostate cancer cells positively correlates with the expression of markers of both cell proliferation and angiogenesis. Although we agree that IL-8 will support tumor growth *in vivo* as a result of regulating tumor vascularity, our data also show that IL-8 exhibits a modest but direct mitogenic effect on prostate cancer cells. The discrepancy with prior studies may lie in the failure to account for the confounding effect of constitutive IL-8 signaling in prostate cancer cells and the absence of pathology studies on human tissue to guide *in vitro* investigation. The detection of intracellular IL-8 and that of its receptors in prostate cancer cells *in vivo* has focused our attention on elucidating the significance of cytoplasmic retention of IL-8 and its receptors in underpinning the proliferation of prostate cancer cells. Consequently, the role of IL-8 as a mitogen in prostate cancer was only uncovered once we targeted the pharmacologic interventions toward the inhibition of cytoplasmic IL-8 expression or signaling.

IL-8 expression in human prostate biopsy tissue was also correlated with MVD, consistent with previous reports illustrating the correlation of IL-8 expression with angiogenic responses in orthotopic models of prostate cancer in athymic nude mice (1, 2) and the capacity for IL-8 to promote the proliferation and migration of human microvascular cells (22–24).

In conclusion, in contrast to histologically normal epithelium, we have identified the emergence of IL-8 and IL-8 receptor expression within the cytoplasm and on the nonapical part of the cell membrane of cancer cells and cells within foci of high-grade PIN by immunohistochemistry of prostate biopsy tissue. Cytoplasmic and nonapical membrane pattern expression of IL-8 correlated with cell proliferation and angiogenesis. The association of IL-8 expression with cell proliferation was confirmed *in vitro* where the addition of IL-8 increased proliferation in whole-cell assays and activated mitogenic signaling responses in prostate cancer cells. We propose that the altered distribution of this chemokine and its receptors may initiate autocrine signaling loops that may contribute to the transcriptional basis underpinning the progression of PIN to invasive prostate carcinoma and, subsequently, to androgen-independent prostate cancer.

Acknowledgments

We thank Prof. Peter Hall and Drs. Perry Maxwell, Karl Mulligan, and Monica Monaghan (Queens University Belfast, Belfast, Northern Ireland) for providing advice and technical assistance and Drs. David Blakey and Simon Barry (AstraZeneca, Alderley Park, United Kingdom) for providing CXCR2 antagonist, SB225002.

References

1. Inoue K, Slaton JW, Eve BY, et al. Interleukin 8 expression regulates tumorigenicity and metastases in androgen-independent prostate cancer. Clin Cancer Res 2000;6:2104–19.
2. Kim SJ, Uehara H, Karashima T, McCarty M, Shih N, Fidler IJ. Expression of interleukin-8 correlates with angiogenesis, tumorigenicity, and metastasis of human prostate cancer cells implanted orthotopically in nude mice. Neoplasia 2001;3:33–42.
3. Reiland J, Furcht LT, McCarthy JB. CXC-chemokines stimulate invasion and chemotaxis in prostate carcinoma cells through the CXCR2 receptor. Prostate 1999;41:78–88.
4. Veltri RW, Miller MC, Partin AW, Poole EC, O'Dowd GJ. Interleukin-8 serum levels in patients with benign prostatic hyperplasia and prostate cancer. Cancer 1999;91:2322–8.
5. McCarron SL, Edwards S, Evans PR, et al. Influence of cytokine gene polymorphisms on the development of prostate cancer. Cancer Res 2002;62:3369–72.
6. Lee LF, Louie MC, Desai SJ, et al. Interleukin-8 confers androgen-independent growth and migration of LNCaP: differential effects of tyrosine kinases Src and FAK. Oncogene 2004;23:2197–205.
7. Anderson J, Reddy VB, Green L, et al. Role of expression of cell cycle inhibitor p27 and MIB-1 in predicting

lymph node metastasis in male breast carcinoma. Breast J 2002 Mar-Apr;8:101–7.

8. Weidner N, Semple JP, Welch WR, Folkman J. Tumor angiogenesis and metastasis-correlation in invasive breast carcinoma. N Engl J Med 1991;324:1–8.

9. Ferrer FA, Miller LJ, Andrawis RI, et al. Angiogenesis and prostate cancer: *in vivo* and *in vitro* expression of angiogenesis factors by prostate cancer cells. Urology 1998;51:161–7.

10. Moore BB, Arenberg DA, Stoy K, et al. Distinct CXC chemokines mediate tumorigenicity of prostate cancer cells. Am J Pathol 1999;154:1503–12.

11. Aaltomaa S, Eskelinen M, Lipponen P. Expression of cyclin A and D1 proteins in prostate cancer and their relation to clinopathological variables and patient survival. Prostate 1999;38:175–82.

12. Drobnjak M, Osman I, Scher HI, Fazzari M, Cordon-Cardo C. Overexpression of cyclin D1 is associated with metastatic prostate cancer to bone. Clin Cancer Res 2001;6:1891–5.

13. Barlic J, Khandaker MH, Mahon E, et al. β-Arrestins regulate interleukin-8-induced CXCR1 internalization. J Biol Chem 1999;274:16287–94.

14. Prado GN, Suzuki H, Wilkinson N, Cousins B, Navarro J. Role of the C-terminus of the interleukin-8 receptor in signal transduction and internalization. J Biol Chem 1996;271:19186–90.

15. Ludwig A, Ehlert JE, Flad H-D, Brandt E. Identification of distinct surface-expressed and intracellular CXC-chemokine receptor 2 glycoforms in neutrophils: *N*-glycosylation is essential for maintenance of receptor surface expression. J Immunol 2000;165:1044–52.

16. Takamori H, Oades ZG, Hoch OC, Burger M, Schraufstatter IU. Autocrine growth effect of IL-8 and GROα on a human pancreatic cancer cell line, Capan-1. Pancreas 2000;21:52–6.

17. Venkatakrishnan G, Salgia R, Groopman JE. Chemokine receptors CXCR1/2 activate mitogen activated protein kinase via the epidermal growth factor in ovarian cancer cells. J Biol Chem 2000;275:6868–75.

18. Xu L, Fidler IJ. Interleukin 8: an autocrine growth factor for human ovarian cancer. Oncol Res 2000;12:97–106.

19. Li A, Varney ML, Singh RK. Expression of interleukin 8 and its receptors in human colon carcinoma cells with different metastatic potentials. Clin Cancer Res 2001;7:3298–304.

20. Brew R, Erikson JS, West DC, Kinsella AR, Slavin J, Christmas SE. Interleukin-8 as an autocrine growth factor for human colon carcinoma cells *in vitro*. Cytokine 2000;12:78–85.

21. Uzgare AR, Kaplan PJ, Greenberg NM. Differential expression and/or activation of p38 MAPK, Erk1/2 and Jnk during the initiation and progression of prostate cancer. Prostate 2003;55:128–39.

22. Li A, Dubey S, Varney ML, Dave BJ, Singh RK. IL-8 directly enhanced endothelial cell survival, proliferation, and matrix metalloproteinases production and regulated angiogenesis. J Immunol 2003;170:3369–76.

23. Varney ML, Olsen KJ, Mosley RL, Bucana CD, Talmadge JE, Singh RK. Monocyte/macrophage recruitment, activation and differentiation modulate interleukin-8 production: a paracrine role of tumor-associated macrophages in tumor angiogenesis. In Vivo 2002;16:471–7.

24. Li A, Dubey S, Varney ML, Singh RK. Interleukin-8-induced proliferation, survival, and MMP production in CXCR1 and CXCR2 expressing human umbilical vein endothelial cells. Microvasc Res 2002;64:476–81.